Prediction of residual stresses in girth welded pipes using an artificial neural network approach

Accepted Manuscript

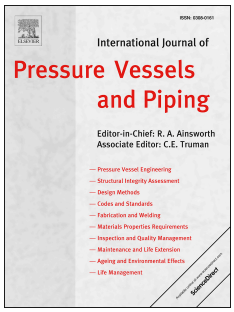

Prediction of residual stresses in girth welded pipes using an artificial neural network approach

J. Mathew, R.J. Moat, S. Paddea, M.E. Fitzpatrick, P.J. Bouchard

PII: S0308-0161(15)30097-1

DOI: 10.1016/j.ijpvp.2017.01.002

Reference: IPVP 3594

To appear in: *International Journal of Pressure Vessels and Piping*

Received Date: 13 October 2015

Revised Date: 17 January 2017

Accepted Date: 25 January 2017

Please cite this article as: Mathew J, Moat RJ, Paddea S, Fitzpatrick ME, Bouchard PJ, Prediction of residual stresses in girth welded pipes using an artificial neural network approach, *International Journal of Pressure Vessels and Piping* (2017), doi: 10.1016/j.ijpvp.2017.01.002.

Prediction of residual stresses in girth welded pipes using an artificial neural network approach

J. Mathew [a,b*], R. J. Moat [b], S. Paddea [b], M.E. Fitzpatrick [c], P.J. Bouchard [b]

[a] *Now at: Faculty of Engineering and Computing, Coventry University, Priory Street, Coventry CV1 5FB, UK*

[b] *Department of Engineering and Innovation, The Open University, Walton hall, Milton Keynes, MK7 6AA, UK*

[c] *Faculty of Engineering and Computing, Coventry University, Priory Street, Coventry CV1 5FB, UK*

**Corresponding author email address: Jino.Mathew@coventry.ac.uk*

Abstract

Management of operating nuclear power plants greatly relies on structural integrity assessments for safety critical pressure vessels and piping components. In the present work, residual stress profiles of girth welded austenitic stainless steel pipes are characterised using an artificial neural network approach. The network has been trained using residual stress data acquired from experimental measurements found in literature. The neural network predictions are validated using experimental measurements undertaken using neutron diffraction and the contour method. The approach can be used to predict through-wall distribution of residual stresses over a wide range of pipe geometries and welding parameters thereby finding potential applications in structural integrity assessment of austenitic stainless steel girth welds.

Keywords: residual stress profile; girth welds; stainless steel; neural network; neutron diffraction; contour method

1.0 Introduction

Characterisation of residual stress distribution in pressure vessel and piping systems has received increased attention owing to its impact on the economy and safety of operating power plants. The presence of tensile residual stresses induced by welding can have a detrimental effect on the life of the components and may lead to crack initiation and growth, and an increased risk of catastrophic failure by fracture [1]. Residual stresses are generated as a result of some form of displacement misfit; for example owing to differential thermal expansion or localised plastic deformation [2]. Quantifying the magnitude and distribution of residual stresses with high certainty in multi-pass weldments is a challenging task. This is mainly because of the large number of interacting factors such as welding parameters, geometry, composition, microstructure, phase transformations, and the thermal and mechanical properties of the weld and parent materials [3]. The use of finite element computational methods is becoming increasingly popular for prediction of welding induced residual stresses in thick-section components. However, these methods usually involve complex non-linear analyses, and can be biased by the analyst's judgements, inappropriate assumptions, boundary conditions and modelling procedures [4]. Measurement techniques [5, 6] such as deep hole drilling [7], neutron diffraction [8] and the contour method [9] can now provide high quality residual stress data for complex weldments. But such measurements are costly, usually involve partial or full destruction of the component, have uncertainties associated with random and systematic errors. In engineering fracture assessment procedures, the three dimensional residual stress field is usually simplified by considering a representative one dimensional profile along the through-thickness of the stress tensor component acting normal to the crack face [10, 11]. Stress intensity factor is calculated from this estimated through-thickness stress profile and used directly in the fracture assessment. Residual stress profiles using various analytical models have been proposed recently for

austenitic stainless steel girth welds, mainly considering the pipe geometry and welding heat input as the critical input parameters [12], [13] and [14]. In the present work, an artificial neural network (ANN) model has been developed which is trained using historical residual stress measurements to predict through-wall residual stress profiles along the weld-centre line of austenitic stainless steel pipes.

2.0 Materials and methods

Artificial neural networks (ANNs) [15] are employed in multi-variate systems to determine non-linear relationships that can be used to solve problems in pattern recognition. During training, a set of coefficients (known as weights and biases) are optimised using a suitable algorithm such as back-propagation [16] by minimizing an error function. In the recent past, ANNs have been extensively used to solve non-linear problems in materials engineering [17], [18] and [19]. In this study, Multilayer ANNs [20] are applied to predict through-thickness residual stress profiles in circumferentially welded austenitic stainless steel pipes using experimental data for training, previously reported in [12]. Residual stress data used for training were measured using Deep Hole Drilling (DHD), neutron diffraction, and Block Removal Slitting and Layering (BRSL). The validation data set comprises new residual stress measurements (contour method and neutron diffraction) for three butt-welded pipe components (Validation Welds 1, 2 and 3) fabricated from austenitic stainless steel with different electrical heat inputs. A summary of the welding details of training and validation mock-ups are given in Table 1. The process parameter envelope of training and validation data representing the geometry and welding heat input of the girth welds are illustrated in Fig. 1. The welds fabricated for the purpose of validation were characterised by following a standard metallographic procedure. Fig. 2 shows weld macrographs and Vickers hardness (HV5) maps of the three validation welds examined by grinding down to 4000 grit using silicon carbide paper and polishing with diamond suspension. Hardness measurements were

performed using a Vickers (HV) indenter, applying a load of 5 kg, using an automated Struers Duramin-A-300 hardness tester.

2.1 Artificial neural network approach

Historical residual stress measurements were used to train the ANN using a Scaled Conjugate Gradient (SCG) algorithm [21] taking into account the through-wall position, pipe radius and thickness, net heat input (Q = arc efficiency × electrical heat input) and yield strength of the material (see Fig. 3). The input parameters were simplified considering the dimensionality phenomenon [22], of training data which can otherwise increase exponentially with the dimensionality of associated input space. Experimental measurements were performed in components fabricated from austenitic stainless steel using various welding processes with net heat input (Q = 0.8-2.2 kJ/mm), wall thickness (t = 16-110 mm) and pipe mean radius to thickness ratio (R/t = 1.8-25) by the UK nuclear industry in order to validate a series of residual stress predictions using the finite element method. All residual stress measurement techniques have limitations and associated uncertainties. For example BRSL has low spatial resolution, neutron diffraction is very dependent on obtaining reliable stress-free lattice parameter data (which can be challenging for weld metal where the composition, texture and grain size vary) and DHD has limited spatial resolution and the specific technique used at that time was susceptible to plasticity induced errors. The uncertainties associated with the historical data are judged to be in the order of ± 50 MPa.

An ensemble of networks having the multi-layer perceptron architecture was implemented in the neural network toolbox in MATLAB [23]. The network's non-linear capability was realised by using the log-sigmoid transfer function in the first layer, and a linear function in the second layer. Equation (1) denote the output y from the second layer as,

$$y = \sum_{j=1}^{H} w_j \mathrm{logh}\left[\sum_{i=1}^{4} w_{ji} p_i + b^{(1)}\right] + b^{(2)} \tag{1}$$

where w_j was the weight vector of the output layer, w_{ji} weight vector of the hidden layer, $b^{(2)}$ bias vector of the output layer, $b^{(1)}$ bias vector of the hidden layer, H the number of hidden nodes, p the scalar input and i the number of inputs. Input variables were normalised to a value between –1 and 1 by using the transformation; Normalised input = 2 × (input – minimum input) / (maximum input – minimum input) – 1. An ensemble of networks was constituted by running 1024 independent training iterations with the weights initialised randomly on the error surface. The Bayesian Error function $E(w)$ was used to evaluate the generalisation ability of the network defined by equation (2),

$$E(w) = \alpha E_R + \beta E_S \tag{2}$$

where α and β are the objective function parameters controlling weight decay and the variance in noise, w is the weight matrix, x the target vector, p the input variables, and o the output.

$$E_S = \frac{1}{2}\sum_{i=1}^{N}\{x - o(p,w)\}^2 \tag{3}$$

$$E_R = \frac{1}{2}\sum_{i=1}^{R}\left|w_i\right|^2 \tag{4}$$

The regularisation term E_R limits the network weights and biases to small values thereby decreasing the susceptibility of the model to over-fitting. The objective function parameters were inferred from the training data and can largely influence the model complexity. The use of over-complex models over simpler models is not justified as it can have an adverse effect on the generalisation ability of the network [24].

2.2 Neutron diffraction

Through-wall residual stress profiles for Validation Welds 1 and 2 (material type: austenitic stainless steel type 316L, dimensions: 250 mm outside diameter, 25 mm thick and 320 mm long) were determined from neutron diffraction measurements. A monochromatic

neutron beam with wavelength 1.648 Å were used by collimating to a nominal gauge volume of $(2.3 \times 2.3 \times 2.3)$ mm^3 at the SALSA beam line [25], Institut Laue Langevin, Grenoble, France. A diffraction angle of approximately 99° was obtained and the {311} reflection was chosen (as being least sensitive to plastic strains). The removed plug of material were used to extract four small cubes of weld metal having dimensions 5 mm × 5 mm × 5 mm to measure the reference stress-free lattice parameter (d_0). Position and direction specific stress-free references were used for calculations by interpolating using a second order polynomial function. The strains, ε, along the three orthogonal directions were calculated from the shift in diffraction peak positions using equation (5),

$$\varepsilon_{(x,\,y,\,z)} = -\frac{\left(\theta - \theta_{0(x,\,y,\,z)}\right) \times \frac{\pi}{360}}{Tan\left(\theta \times \frac{\pi}{360}\right)} \times 1000000 \tag{5}$$

For determining stresses from the measured strains, the material was assumed to be isotropic. Furthermore, the Kröner model was implemented in the DECcalc software [26], to calculate the diffraction elastic constants. A Young's modulus value of 187 GPa and Poisson's ratio of 0.303 were used to determine the stresses in three different orientations from the measured strains using equation (6), (7) and (8),

$$\sigma_{xx} = \frac{E_{311}}{\left(1+\nu_{311}\right)\left(1-2\nu_{311}\right)}\left[\left(1-\nu_{311}\right)\varepsilon_{xx} + \nu_{311}\left(\varepsilon_{yy} + \varepsilon_{zz}\right)\right] \tag{6}$$

$$\sigma_{yy} = \frac{E_{311}}{\left(1+\nu_{311}\right)\left(1-2\nu_{311}\right)}\left[\left(1-\nu_{311}\right)\varepsilon_{yy} + \nu_{311}\left(\varepsilon_{xx} + \varepsilon_{zz}\right)\right] \tag{7}$$

$$\sigma_{zz} = \frac{E_{311}}{\left(1+\nu_{311}\right)\left(1-2\nu_{311}\right)}\left[\left(1-\nu_{311}\right)\varepsilon_{zz} + \nu_{311}\left(\varepsilon_{xx} + \varepsilon_{yy}\right)\right] \tag{8}$$

2.3 Contour method

The contour method, a destructive technique to determine residual stresses was applied to Validation Welds 1 and 2 after the neutron diffraction measurement, and to measure both axial and hoop stresses in Validation Weld 3 (material type: Esshete 1250, dimensions: 180 mm outside diameter, 35 mm thick and 200 mm long). The contour method can be applied to provide a full 2-D cross sectional map of the hoop residual stresses present in thick cylindrical components [27]. In this method, the component of interest is cut into two halves using wire electric discharge machining, the deformation contours of the relaxed cut surfaces measured, the matching profiles averaged (to eliminate shear effects) and then applied as a boundary condition to the cut face of one half of the cut component in a linear elastic finite element analysis. The distribution of hoop stress of the component of interest can be determined by performing a cut along a radial-axial plane using the approach reported [28], by cutting the pipe lengthways into two halves using wire electro discharge machining severing both the opposite thicknesses simultaneously. The axial stress residual profiles were determined along different through-thickness positions at 36°, 90° and 144° with respect to the flat edge (XX) in the clockwise direction and averaged across 45° on either sides of the normal YY as shown in Fig. 4a. In order to determine the axial stresses, a second cut was performed along the radial-hoop plane XY (see Fig. 4b) at the centre of the weld. The data analysis procedure was similar to the hoop residual stress measurement with additional steps implemented to account for the stress relaxation effects from the previous cut (along XZ plane) by applying displacement boundary conditions of the finite element model created for measuring the hoop stresses.

3.0 Results and Discussion

A histogram was developed to manage scatter within the neural network predictions and to provide a reliable prediction interval of the estimated stress distributions. The 10% of

predictions with lowest error were determined from a committee of 1024 networks with the histogram of output distribution divided into 25 segments. Model predictions expressed as a contour plot generated from the histograms of network outputs (red and white colour represents the most and least probable region of predictions) are compared with the new experimental measurements (i.e. Validation Welds 1, 2 and 3) to assess the performance of the ANN. In Fig. 5(a) the ANN prediction for residual stresses in the axial direction of Validation Weld 1 is compared with neutron measurements. The agreement with measurements is good considering the scatter observed in the measured data. Fig. 5(b) shows the ANN prediction for hoop stresses compared with validation measurements made by neutron diffraction and the contour method, the latter for both top and bottom of the pipe. Agreement between the experimental validation measurements is excellent. However, the ANN prediction is substantially more tensile towards the inside diameter of the pipe. The presence of high compressive stresses near the inside surface is likely to be the result of the specific weld procedure employed for Validation Welds 1 and 2 (see Fig. 2(a) and (b)); that is an unusually wide weld preparation was used with a backing plate and weld joint closed up to nearly one half of its initial width during welding. This may have introduced unusually high compressive hoop stresses in these welds which were beyond the envelope of the training data. The ANN method only predicts based on the training data used, therefore this result is unsurprising, given that the stress profile of Validation Weld 1 is to some extent non-representative of previously seen data. The inability to extrapolate beyond the boundaries of the training data is a key limitation of the ANN method. Despite this the ANN is in favourable agreement with the measurements from mid thickness to the outer radius position, and over-predicts the tensile magnitude of stress at all positions.

Predicted and measured residual stress profiles in the axial and hoop directions for Validation Weld 2 are shown in Fig. 6 (a) and (b) respectively. The ANN histogram map is in reasonable

agreement with the neutron measurements in the axial direction up to the through-wall position $x/t = 0.7$. However the hoop stress measurements deviate from the ANN map for $x/t < 0.3$ in the same manner as Validation Weld 2; this is to be expected because the pipe weld was made in the same way as Validation Weld 1 (with a wide weld preparation and backing plate). The hoop stress measurements near the outer surface ($x/t > 0.7$) are noticeably lower than the contour measurements which closely follow the ANN predictions. A similar trend is observed in the axial stress measurements approaching the outer radius of the weld. The lower than expected magnitude of axial and hoop stresses measured by neutron diffraction for $x/t > 0.7$ may be associated with uncertainties in stress-free lattice parameter measurements for austenitic weld metal owing to compositional variations, texture and large grain size effects [6, 8]. But the consistency of the neural network predictions is verified by the contour method measurements carried out in the hoop direction (Fig. 6b). The axial stress profiles measured using the contour method at various positions (Fig. 7a) are in good agreement with the ANN prediction up to $x/t < 0.8$ and the latter imply the presence of higher tensile stresses approaching the outer surface. The mismatch in predicted and measured stress distribution close to the outer surface is likely to be associated with a lower density of surface measurement data used to train the ANN. Additionally the hoop stress profiles predicted by the ANN approach for Validation Weld 3 are in reasonable agreement with the measurements made using the contour method (see Fig. 7b).

Interestingly, the ANN model rarely under-predicts the magnitude of the measured tensile stress by a large margin in the validation dataset. This is a useful characteristic if ANN residual stress profiles are to be used in safety critical assessments of welded structures [10]. The advantage of the ANN method for defining through-wall residual stress profiles compared with computational weld mechanics or measurement approaches is that the information required to train the model is straightforward and historical measured data can be

used. On the contrary, the ANN provide somewhat smoothed residual stress profile and are unable to capture the stress variations through the thickness especially in comparison with neutron diffraction data. However, this limitation is considered to be the consequence of using insufficient neutron data in training and an improved database with more neutron measurements is recommended for the application of the model. Another drawback is that the weldment for which a prediction is to be made must fall within the range of weld types used to train the model.

4.0 Conclusions

To summarise, an artificial neural network model was developed to characterise the through-thickness distribution of residual stresses in circumferentially welded austenitic stainless steel pipes, providing the weldment type lies within the boundary of the training data envelope used. The model has been validated by comparing predicted profiles with new experimental measurements for three welded pipes constructed using different process parameters. The model has the potential to be developed into a tool for characterising residual stress profiles in different classes of weldment, for example plate butt welds, nozzle welds, laser or electron beam welds, etc. For each class of weldment, geometry, material or stress component a separate ANN can be trained provided sufficient measured data are available.

Acknowledgements

The authors are grateful for funding received from EDF Energy, AMEC Power and Process Europe, and the Lloyd's Register Foundation. The award of neutron beamtime by the Institut Laue-Langevin (ILL) is also gratefully acknowledged. Michael Fitzpatrick and Jino Mathew are funded by the Lloyd's Register Foundation (LRF), a charitable foundation helping to protect life and property by supporting engineering-related education, public engagement and the application of research.

References

[1] Withers PJ. Residual stress and its role in failure, Reports Prog. Phys. 2007; 70: 2211–64. doi:10.1088/0034-4885/70/12/R04.

[2] Withers PJ, Bhadeshia HKDH. Residual stress Part 2 – Nature and origins, Mater. Sci. Technol. 2001; 366-75.

[3] Leggatt RH. Residual stresses in welded structures, Int. J. Press. Vessel. Pip. 2008; 85: 144–51. doi:10.1016/j.ijpvp.2007.10.004.

[4] Smith MC, Bouchard PJ, Turski M, Edwards L, Dennis RJ. Accurate prediction of residual stress in stainless steel welds, Comput. Mater. Sci. 2012; 54: 312–28. doi:10.1016/j.commatsci.2011.10.024.

[5] Withers PJ, Bhadeshia HKDH. Residual stress Part 1 – Measurement techniques, Mater. Sci. Technol. 2001; 17: 355–365.

[6] Schajer GS, Practical Residual Stress Measurement Methods, John Wiley & Sons, Ltd.; 2013.

[7] George D, Kingston E, Smith DJ. Measurement of through-thickness stresses using small holes, J. Strain Anal. Eng. Des. 2002; 37: 125–39.

[8] Hutchings, MT, Withers PJ, Holden, TM, Lorentzen T, Introduction to characterization of residual stress by neutron diffraction, Taylor & Francis; 2005. doi:10.1016/S1369-7021(05)00849-7.

[9] Prime MB. Cross-Sectional Mapping of Residual Stresses by Measuring the Surface Contour After a Cut, J. Eng. Mater. Technol. 2001; 123 (2): 162-68. doi:10.1115/1.1345526.

[10] Procedure R6 Revision 4, Assessment of the integrity of structures containing defects; EDF Energy Ltd; 2013

[11] API RP 579-1/ASME FFS-1. Houston, TX: American Petroleum Institute; August 2007.

[12] Bouchard PJ. Validated residual stress profiles for fracture assessments of stainless steel pipe girth welds, Int. J. Press. Vessel. Pip. 2007; 84: 195–222. doi:10.1016/j.ijpvp.2006.10.006.

[13] Dong P, Song S, Zhang J, Kim MH. On residual stress prescriptions for fitness for service assessment of pipe girth welds, Int. J. Press. Vessel. Pip. 2014; 123-124: 19–29. doi:10.1016/j.ijpvp.2014.07.006.

14] Song S, Dong P, Pei X. A full-field residual stress estimation scheme for fitness-for-service assessment of pipe girth welds: Part I – Identification of key parameters, Int. J. Press. Vessel. Pip. 2015; 126-127: 58–70. doi:10.1016/j.ijpvp.2015.01.002.

[15] Bishop CM. Neural Networks for Pattern Recognition, Oxford University Press; 1997.

[16] Rumelhart DE, Hinton GE, Williams RJ. Learning representations by back-propagating errors, Nature 1986; 323: 533–36.

[17] Toktaş İ, Özdemir AT. Artificial neural networks solution to display residual hoop stress field encircling a split-sleeve cold expanded aircraft fastener hole, Expert Syst. Appl. 2011; 38: 553–63. doi:10.1016/j.eswa.2010.06.102.

[18] Na MG, Kim JW, Lim DH. Prediction of Residual Stress for Dissimilar Metals Welding At Nuclear Power Plants Using Fuzzy Neural Network Models, Nucl. Eng. Technol. 2007; 39: 337–48. doi:10.5516/NET.2007.39.4.337.

[19] Yescas M, Bhadeshia, HKDH, Mackay D. Estimation of the amount of retained austenite in austempered ductile irons using neural networks, Mater. Sci. Eng. A. 2001; 311: 162–73. doi:10.1016/S0921-5093(01)00913-3.

[20] Rosenblatt F. The perceptron: a probabilistic model for information storage and organization in the brain., Psychol. Rev. 1958; 65: 386–408. doi:10.1037/h0042519.

[21] Møller M. A scaled conjugate gradient algorithm for fast supervised learning, Neural Networks. 1993; 6: 525–33. doi:10.1016/S0893-6080(05)80056-5.

[22] Bellman RE. Adaptive control processes, Princeton university; 1961.

[23] MATLAB and Neural Network Toolbox Release 2012a, The MathWorks Inc., Natick, Massachusetts, United States.

[24] Mackay, D. Bayesian methods for Adaptive models, California Institute of technology; 1991.

[25] Pirling T, Bruno G, Withers PJ. SALSA, a new concept for strain mapping at the ILL, Mater. Sci. Eng. A. 2006; 437: 139–44.

[26] Manns TM, Scholtes B. DECcalc - A software for the calculation of diffraction elastic constants from single crystal coefficients, Mater. Sci. Forum 2011; 681: 417-19.

[27] Pagliaro P, Prime MB, Robinson JS, Clausen B, Measuring Inaccessible Residual Stresses Using Multiple Methods and Superposition, Exp. Mech. 2011; 51(7): 1123-34.doi:10.1007/s11340-010-9424-5.

[28] Hosseinzadeh F, Bouchard, PJ. Mapping Multiple Components of the Residual Stress Tensor in a Large P91 Steel Pipe Girth Weld Using a Single Contour Cut, Exp. Mech. 2012; 53: 171–81. doi:10.1007/s11340-012-9627-z.

Figure and table captions

Table 1. Welding details of training and validation mock-ups

Fig. 1. Process parameter envelope of training and validation data with respect to net heat input, component thickness (t) and marker colour denoting R/t ratio (VW 1, VW 2 and VW 3 corresponding to Validation Weld 1, 2 and 3 respectively).

Fig. 2. Weld macrograph (on the left) and Vickers hardness (HV5) map (right) of (a) Validation Weld 1 (b) Validation Weld 2, and (c) Validation Weld 3.

Fig. 3. Schematic of the ANN architecture used in this study; Input parameters t, R/t, x/t and Q denote the pipe wall thickness, mean radius over thickness ratio, through thickness position from inner surface and net heat input (Q = arc efficiency × electrical heat input) respectively.

Fig. 4. Schematic illustration of (a) through-thickness measurement locations in Validation Weld 3 (b) location and direction of the performed contour cuts.

Fig. 5. ANN model prediction of (a) axial stresses (on the left) and (b) hoop stresses (on the right) compared with experimental measurements for Validation Weld 1.

Fig. 6. ANN model prediction of (a) axial stresses and (b) hoop stresses compared with experimental measurements for Validation Weld 2.

Fig. 7. ANN model prediction of (a) axial stresses and (b) hoop stresses compared with experimental measurements for Validation Weld 3.

Table 1. Welding details of training and validation mock-ups

Mock-ups	Welding Process	Net Heat Input (kJ/mm)	Welding passes	Yield stress (p, w)* (MPa)	Groove type
Training					
1	SAW	2.2	4	338, 476	Double V
2	MMAW	1.12	16	272, 446	Outer J
3	MMAW	1.68	26	328, 446	Outer J
4	MMAW	1.92	44	328, 446	Outer J
5	MMAW	1.12	A	328, 446	Outer J
6	MMAW	0.8	A	328, 446	Outer J
7	TIG	1.32	A	328, 446	Narrow gap
8	SAW	1.8	84	274, 483	Outer J
Validation					
1	TIG	0.9	108	300, 500	Wide Single V
2	TIG	1.8	58	300, 500	Wide Single V
3	TIG, MMAW	1.5	25	370, 564	Single V

*where p, w are the parent and weld material yield strength at 1% proof stress. a - passes unknown.

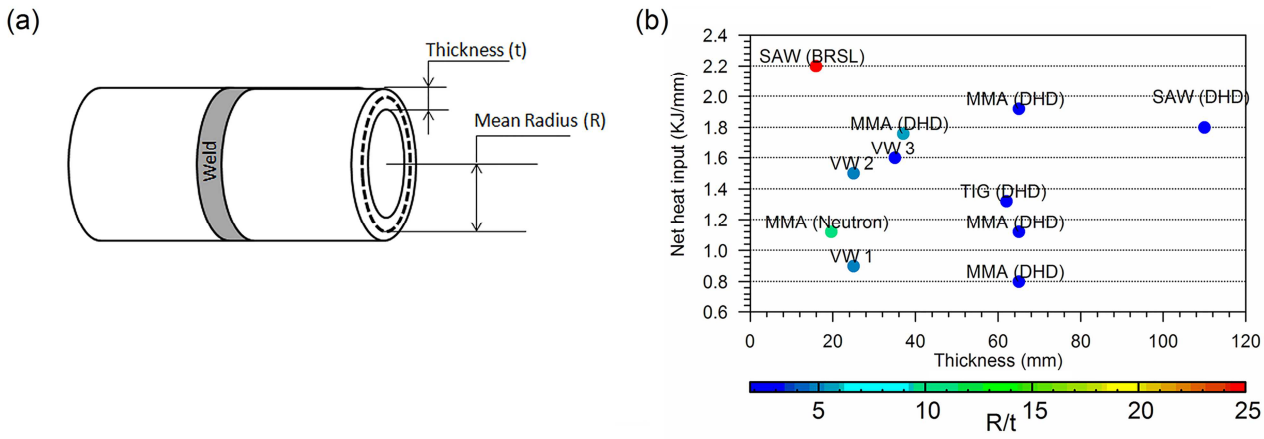

Fig. 1. (a) Schematic of the pipe girth weld geometry for training and validation residual stress measurement data, and (b) process parameter envelope of training and validation data with respect to net heat input, component thickness (t) and marker colour denoting R/t ratio (VW 1, VW 2 and VW 3 corresponding to Validation Weld 1, 2 and 3 respectively).

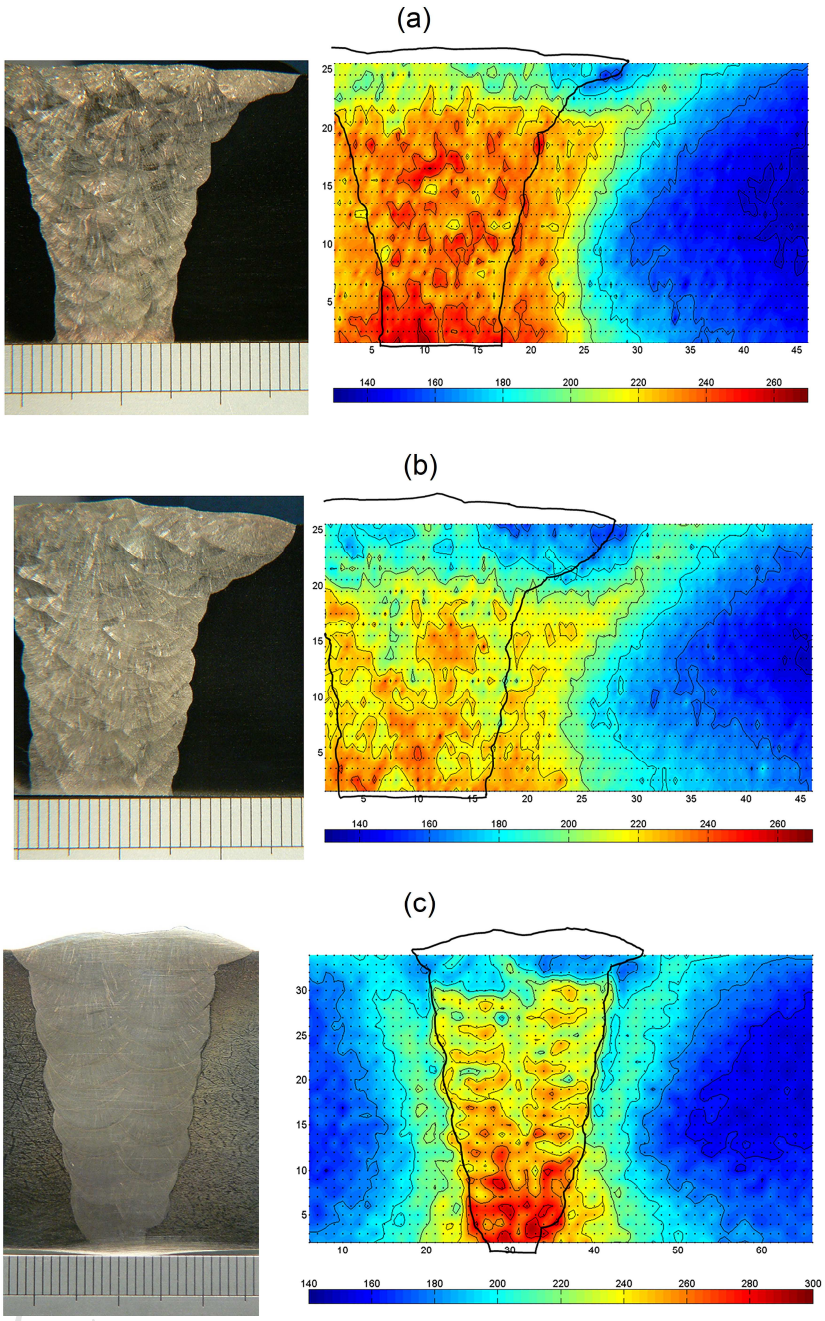

Fig. 2. Weld macrograph (on the left) and Vickers hardness (HV5) map (right) of (a) Validation Weld 1 (b) Validation Weld 2, and (c) Validation Weld 3.

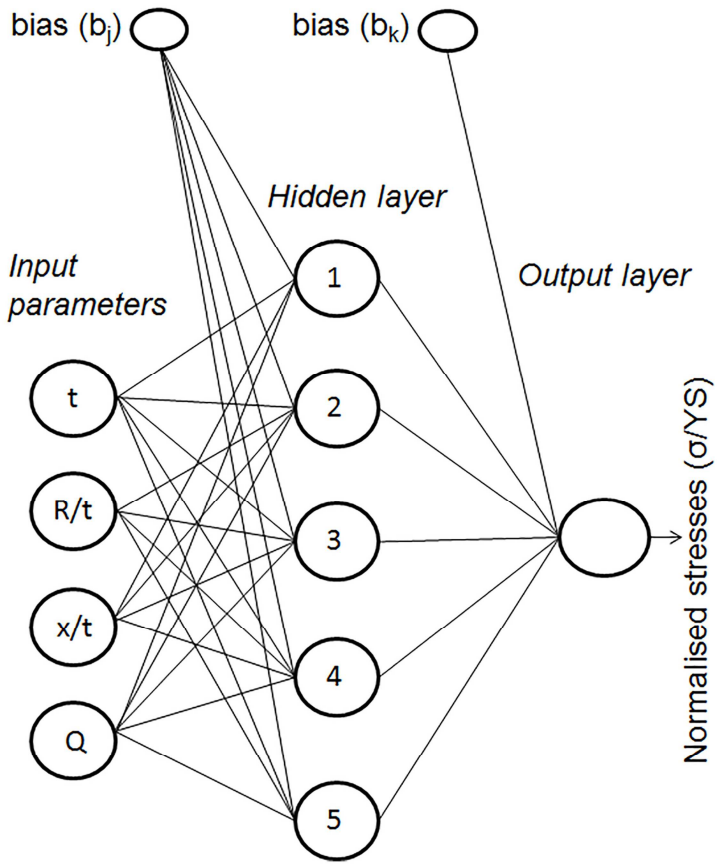

Fig. 3. Schematic of the ANN architecture used in this study; Input parameters t, R/t, x/t and Q denote the pipe wall thickness, mean radius over thickness ratio, through thickness position from inner surface and net heat input (Q = arc efficiency × electrical heat input) respectively. Normalised stresses (denoted as σ/YS) is predicted as the output where σ stands for the predicted stress along axial or hoop direction, and YS represents the yield strength at 1% proof stress.

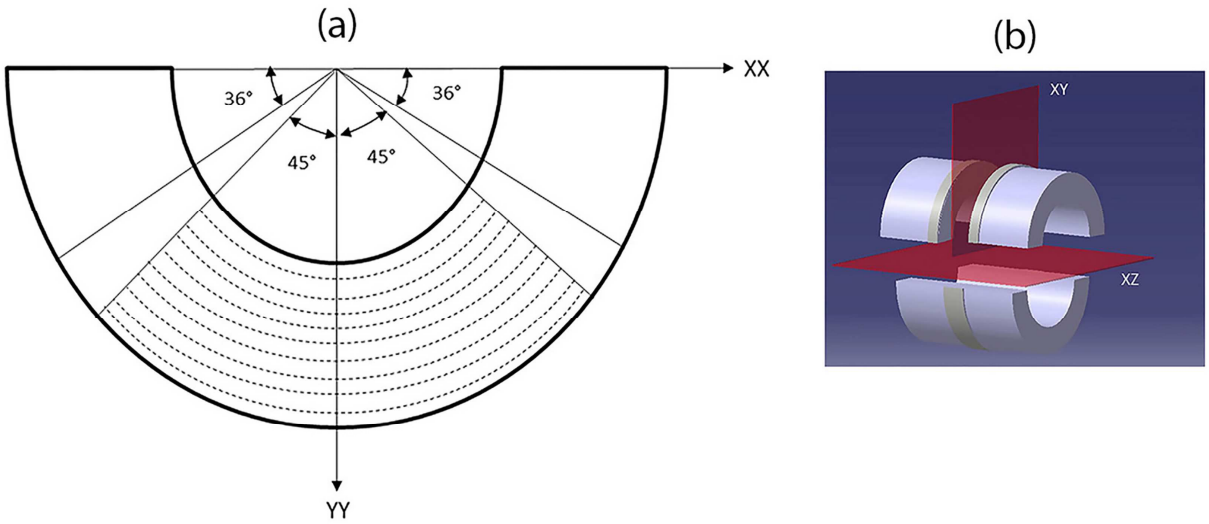

Fig. 4. Schematic illustration of (a) through-thickness measurement locations in Validation Weld 3 (b) location and direction of the performed contour cuts.

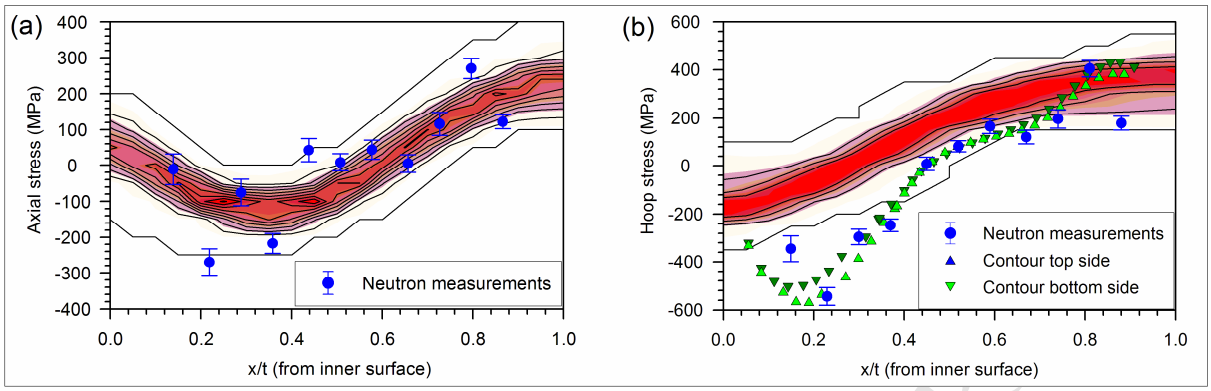

Fig. 5. ANN model prediction of (a) axial stresses (on the left) and (b) hoop stresses (on the right) compared with experimental measurements for Validation Weld 1.

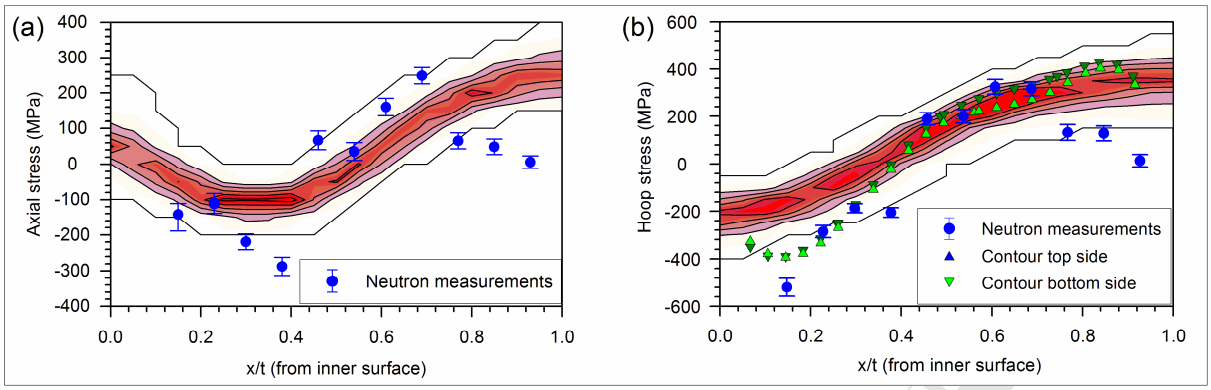

Fig. 6. ANN model prediction of (a) axial stresses and (b) hoop stresses compared with experimental measurements for Validation Weld 2.

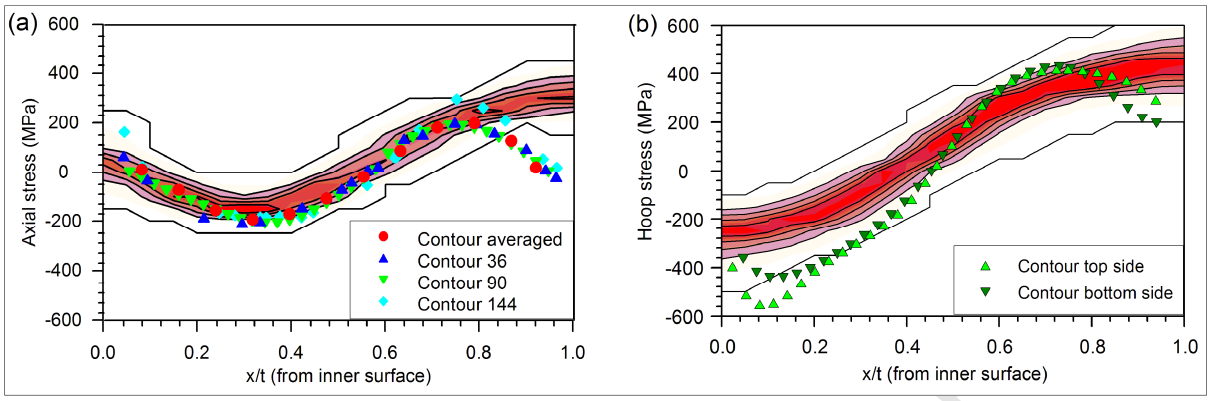

Fig. 7. ANN model prediction of (a) axial stresses and (b) hoop stresses compared with experimental measurements for Validation Weld 3.

Highlights

We model residual stresses in multi-pass girth welds using artificial neural networks.

We validated the model with experimental measurements using neutron diffraction and contour method.

A histogram network was developed to provide a reliable prediction interval of the estimated stress distributions.

The model can function providing the weldment type lie within the boundary of the training data envelope used.

ANN model can find potential applications in the structural integrity assessment of weldments.